

Lattice calculation of 1^{-+} hybrid mesons with improved Kogut-Susskind fermions

C. Bernard

Department of Physics, Washington University, St. Louis, MO 63130, USA

T. Burch, E.B. Gregory, and D. Toussaint

Department of Physics, University of Arizona, Tucson, AZ 85721, USA

C. DeTar and J. Osborn

Physics Department, University of Utah, Salt Lake City, UT 84112, USA

Steven Gottlieb

Department of Physics, Indiana University, Bloomington, IN 47405, USA

U.M. Heller

American Physical Society, One Research Road, Box 9000, Ridge, NY 11961-9000

R. Sugar

Department of Physics, University of California, Santa Barbara, CA 93106, USA

(Dated: October 31, 2018)

Abstract

We report on a lattice determination of the mass of the exotic 1^{-+} hybrid meson using an improved Kogut-Susskind action. Results from both quenched and dynamical quark simulations are presented. We also compare with earlier results using Wilson quarks at heavier quark masses. The results on lattices with three flavors of dynamical quarks show effects of sea quarks on the hybrid propagators which probably result from coupling to two meson states. We extrapolate the quenched results to the physical light quark mass to allow comparison with experimental candidates for the 1^{-+} hybrid meson. The lattice result remains somewhat heavier than the experimental result, although it may be consistent with the $\pi_1(1600)$.

PACS numbers: 11.15Ha, 12.38.Gc

I. INTRODUCTION

The fact that gluons carry color charge suggests that they, like quarks, could be “valence” constituents of hadrons. In other words, we expect that the spectrum of QCD should contain glueballs and hybrids, or particles with both quarks and gluons as valence constituents. Hybrid mesons can have exotic quantum numbers, or J^{PC} combinations not possible with a quark-antiquark state. However, a state with exotic quantum numbers is not necessarily a hybrid — it could be a $\bar{q}q\bar{q}q$ state, realized either as a single “bag” containing four quarks or as a “molecule” made of two $\bar{q}q$ mesons. Experimental evidence suggests the existence of one or more mesons with exotic quantum numbers $J^{PC} = 1^{-+}$, namely the $\pi_1(1400)$ [1] and the $\pi_1(1600)$ [2]. Analytic and numerical methods to predict the mass of light hybrid meson states include flux tube models [3], the bag model [4, 5, 6, 7, 8], QCD spectral sum rules [9, 11, 12], relativistic WKB calculations [10], and lattice QCD. Several lattice studies [13, 14, 15] have used quenched Wilson or quenched Wilson-clover fermions to calculate the masses of exotic hybrid states, although with quark masses much larger than the physical u and d quark masses. Lacock and Schilling have done a calculation in two flavor QCD, again with fairly heavy quarks [16].

Here we report results of a lattice calculation of the mass of a 1^{-+} hybrid meson using improved Kogut-Susskind quarks. The use of Kogut-Susskind quarks allows us to work at valence quark masses much smaller than were used in previous lattice calculations. In addition, the “ a_{tad}^2 ” action that we use has leading lattice spacing errors of order a^2g^2 , while the clover-Wilson action has errors of order a^2 . Our mass estimates in the quenched approximation are consistent with earlier Wilson quark results, but extrapolation to the physical light valence quark masses is under much better control. Preliminary results of this calculation were reported in Ref. [17].

We have also calculated hybrid meson propagators including the effects of three flavors of dynamical quarks, with light sea quark masses down to 0.4 times the strange quark mass. We find that extracting mass estimates from the propagators in full QCD is difficult, and we argue that this difficulty is due to mixing of the hybrid meson with two meson states — the states into which it might decay.

II. 1^{-+} HYBRID MESON OPERATOR

We can construct a 1^{-+} hybrid meson operator as the cross product of a color octet 1^{--} quark-antiquark (ρ meson) operator and the chromomagnetic field, which has $J^{PC} = 1^{+-}$: $\rho \times B$ [14]. With staggered quarks we have several choices of rho meson operators, but it is convenient to choose the taste 1 singlet ρ_s , with the spin \otimes taste structure $\gamma_i \otimes \mathbf{1}$.

$$\begin{aligned} 1_i^{-+} &= \epsilon_{ijk} \bar{\psi}^a \gamma_j \otimes \mathbf{1} \psi^b B_k^{ab} \\ &= 2 \bar{\psi}^a \gamma_j \otimes \mathbf{1} \psi^b F_{ij}^{ab} \quad , \end{aligned} \quad (1)$$

where i, j and k are spatial indices and a and b are color indices. Each spin component of the 1^{-+} includes two terms, for example:

$$1_x^{-+} = \rho_y B_z - \rho_z B_y \quad , \quad (2)$$

so if we had chosen a spin \otimes taste structure like $\gamma_i \otimes \gamma_i$ the two components of 1_x^{-+} would have different tastes.

The Kogut-Susskind ρ_s meson operator, with spin aligned in the k direction is $\bar{\chi} \eta_k D_k \chi$, [18] where χ and $\bar{\chi}$ are the quark and antiquark fields respectively. The covariant symmetric shift operator is given by

$$D_\mu q(x) = \frac{1}{2} [U_\mu^\dagger(x - \hat{\mu}) q(x - \hat{\mu}) + U_\mu(x) q(x + \hat{\mu})] \quad . \quad (3)$$

We compute the field strength at each lattice point using the four plaquettes in each plane that have corners at this point, as described in Ref. [14]. In computing the field strength, we use links that have been smoothed with 32 iterations of APE smearing in the spatial directions only with relative weight of the staples set to 0.25 [19]. This smearing removes short wavelength fluctuations in the gluon field, and reduces the noise in the hybrid propagator. (The smeared links are only used in constructing $F_{\mu\nu}$; the propagators are computed using the original links.)

Our zero momentum hybrid source and sink wave functions are constructed in Coulomb gauge and consist of a product of quark and antiquark fields with phases and offsets appropriate to a color octet ρ_s , as described above, and multiplied by the smeared field strength

¹ We use the term “taste” to refer to the four types of quarks that are naturally present in the Kogut-Susskind formulation, while “flavor” can also distinguish quarks with an additional externally imposed label. For example, a meson with a source operator $\bar{\psi} \gamma_5 \otimes \mathbf{1} \psi$ but with disconnected diagrams not included would be a taste singlet but flavor non-singlet, and would be a pion in the continuum limit.

symmetrized with respect to the positions of the quark or antiquark to form the required C even combination, as illustrated in Fig. 1:

$$\bar{\chi}\epsilon_{ijk}(\eta_i D_i B_j + B_j \eta_i D_i)\chi \quad (4)$$

The operator is summed over all spatial sites and a trace is taken over the color indices.

The algorithm for constructing the meson propagator starts in Coulomb gauge with a quark “wall source”, consisting of a unit color vector field in a spatially constant direction, and applies the hybrid meson operator to form a source for the antiquark propagator. The calculation of the meson propagator is completed by acting upon the resulting antiquark propagator at an arbitrary time slice by the same hybrid operator and joining the resulting color vector field with the quark field propagated from the same wall source, summing over all sink spatial sites and color indices. The whole process is repeated, summing over the three wall source colors.

III. SIMULATION AND MEASUREMENT

We measured the connected correlator of the 1^{-+} hybrid state on three sets of $28^3 \times 96$ lattices generated with the “ a_{tad}^2 ” action [20]. To isolate the effects of dynamical quarks, we used matched quenched and full QCD lattices with $10/g^2 = 8.40$, $m_{\text{val}}a = 0.016, 0.04$, for the quenched quarks, $10/g^2 = 7.18$ for lattices with three degenerate flavors of dynamical sea quarks at the strange quark mass ($ma = 0.031$) and $10/g^2 = 7.11$ for lattices with $m_{u,d} = 0.4m_s$ ($ma = 0.0124$). These choices of $10/g^2$ give approximately the same lattice spacing (~ 0.09 fm) in the three cases. The corresponding choices of quark mass allow simulation at roughly equivalent values of $(m_{\text{PS}}/m_V)^2$, the square of the ratio of the pseudoscalar to vector meson masses. Table I summarizes the simulation parameters and fit results for the 1^{-+} states, while Table II contains estimates for conventional hadron masses at these parameters.

The size of the datasets is comparable for quenched and full QCD runs. Successive full QCD lattices are separated by six molecular dynamics trajectories, with each trajectory one simulation time unit long. The full QCD lattices are not completely decorrelated but this autocorrelation has negligible effects on the hybrid mass fittings, since hybrid propagators have much larger statistical errors than, e.g. pion propagators. In particular, for the lightest sea and valence quark mass, $am_q = 0.0124$, we calculated the normalized autocorrelations of

the 1^{-+} propagators separated by six simulation time units at each Euclidean time separation, or distance between the wall source and sink. For propagation distances zero through eight with the sample of 532 lattices we find 0.01, 0.13, -0.05, -0.00, 0.08, 0.01, -0.04, -0.16 and -0.08 respectively, instead of the uniformly positive autocorrelations that we would see if the propagators were systematically correlated from one stored lattice to the next. Although the statistical errors we quote come from the covariance matrix of the propagator, we have also performed a jackknife error analysis of each fitted mass and found jackknife error estimates to be consistent with errors from the covariance matrix. Varying the block size from 1 to 10 had no significant effect on the jackknife error.

In a separate study we have measured propagators of the pion, rho and nucleon. Statistical errors on these propagators are much smaller than for the 1^{-+} propagator, so some effects of autocorrelations can be seen. For the nucleon at mass $am_1 = 0.0124$, which we use for comparison with the hybrid propagators, the data was grouped in blocks of four lattices, or 24 trajectories, before the covariance matrix was computed. Further blocking does not significantly increase the error bars. The fact that the nucleon mass fits have good χ^2 (in fact, better than the quenched nucleon fits) is also evidence that this blocking has removed most of the effects of the autocorrelations.

IV. RESULTS

We fit the measured correlators to the sum of oscillating and normal exponentials:

$$C(t) = A_1 e^{-M_{1^{-+}}t} + A_2 (-1)^t e^{-m_2 t} + A_3 (-1)^t e^{-m_3 t}, \quad (5)$$

where $M_{1^{-+}}$ is the hybrid meson mass of interest and m_2 and m_3 are masses of non-exotic parity partner states which have oscillating correlators in the Kogut-Susskind formulation. In our case the oscillating parity partner is a 1^{++} (a_1) state, which is lighter than the 1^{-+} hybrid, and the oscillating component dominates the correlator at large times. It is therefore essential to include the oscillating state(s) in our fits. We performed both four and five parameter fits. For the four parameter fits, we fix $A_3 = m_3 = 0$, meaning that we include one state of each parity. For the five parameter fits we fix m_2 to an a_1 meson mass determined from propagators with a standard $\bar{q}q$ source operator, and fit for A_2 , m_3 and A_3 . We varied the range of the fit and tried to choose values for $M_{1^{-+}}$ corresponding to

high-confidence fits that were insensitive to D_{\max} and D_{\min} , the limits of the fit range.

For the quenched lattices we were able to fit the propagators with reasonable confidence levels (25-50%) for valence quark masses $ma = 0.016$ and $ma = 0.040$. Figure 2 shows the measured propagator for $ma = 0.016$. Note the oscillating component due to parity partner states. As expected, the oscillating component dominates at large distance, since the parity partner has lower mass than the 1^{-+} . Figure 3 shows mass fits for the quenched lattices for $ma = 0.040$ and $D_{\max} = 15$, with both the two particle (four parameter) and three particle (five parameter) fits. In the mass fit plots, we have included the small confidence level fits to illustrate how adjusting the fit range produces more optimal fits. Figure 4 shows the same plot for $ma = 0.016$. In both plots the three particle fits exhibit a plateau with relatively small error bars ($< 1\%$), demonstrating the stability of the result with respect to variations in the fit range. For the four-parameter fits, there is a slight oscillation of fitted values about the same plateau. Furthermore, the range of fits with high confidence level and relatively small errors is reduced. From plots like these, we picked a “best fit”, a value that met some balance of the following criteria: insensitivity to fit range, high confidence level, reasonable statistical errors. We can see that one might reasonably choose any one of several points as a “best fit”, and the range of resulting $M_{1^{-+}}$ values is the basis of our estimate of the systematic error coming from the presence of higher mass states in the propagators. In all of these fit summary figures we include unused fits, that do not meet these criteria, say, because of low confidence level, to help illustrate how we selected the optimal fits.

For lattices with three degenerate sea quarks at m_s , we were also able to extract a value for $M_{1^{-+}}$ in reasonable agreement with the quenched result. Four and five parameter fits are shown in Fig. 5. The fits exhibit larger statistical errors than the quenched lattice fits, and a slight dependence on range. The mass estimate in Table I reflects this with significantly larger statistical and systematic error bars than in the quenched case.

The lattices with $m_{u,d} = 0.4m_s$ proved more interesting and difficult. The $1^{-+} - 1^{++}$ propagator for valence mass $am_q = 0.0124$ for this ensemble is shown in Fig. 6. Fits to the 1^{-+} mass for both valence masses are illustrated in Figs. 7 and 8. The fitted mass agrees with those of the quenched and three-flavor results within two standard deviations, but with larger systematic errors, estimated from the dependence on fit range.

In the case of the light valence quark ($ma = 0.0124$), we were unable to say much about the 1^{-+} hybrid mass with any confidence. It is apparent from visual examination of the

$10/g^2$	$m_{\text{sea}}a$	$m_{\text{val}}a$	$a^2\sigma$	r_1/a	N_{configs}	Range aM_{1-+}	c.l.
8.40	—	0.040	0.0499(5)	3.730(7)	416	4–15 1.062(12)(20)	0.27
8.40	—	0.016	0.0499(5)	3.730(7)	416	4–15 0.973(26)(20)	0.49
7.18	0.031	0.031	0.0405(7)	3.829(13)	509	5–15 0.986(30)(30)	0.83
7.11	0.0124, 0.031	0.031	0.0424(9)	3.708(14)	526	6–15 0.911(34)(100)	0.25
7.11	0.0124, 0.031	0.0124	0.0424(9)	3.708(14)	526	na	

TABLE I: Summary of hybrid meson simulation parameters and results. All lattices have dimensions $28^3 \times 96$. The 1^{-+} (hybrid) mass fits are all three particle fits. The second error on the hybrid mass estimates is an estimate of the possible systematic error from our choice of fit range.

$10/g^2$	$m_{\text{sea}}a$	$m_{\text{val}}a$	aM_{PS}	aM_{V}	aM_{N}	aM_{dec}
8.40	—	0.040	0.348	0.523(3)	0.771(2)	0.855(17)
8.40	—	0.016	0.223	0.468(3)	0.633(2)	0.749(18)
7.18	0.031	0.031	0.320	0.478(1)	0.699(1)	0.766(2)
7.11	0.0124, 0.031	0.031	0.326	0.479(2)	0.710(2)	na
7.11	0.0124, 0.031	0.0124	0.206	0.414(2)	0.579(3)	0.692(4)

TABLE II: Preliminary values for conventional hadron masses at the hybrid mass simulation parameters. Statistical errors on the pseudo-scalar meson mass, aM_{PS} are smaller than the precision shown. Pseudo-scalar and vector meson masses for the $10/g^2 = 8.4$ quenched points were obtained from interpolation or extrapolation from results at valence masses 0.015 and 0.030.

propagator (Fig. 6) that there is a lessening of the overall slope, suggesting that the non-oscillating piece may not be consistent with a single exponential. Indeed, the fits were very range dependent. Together these factors indicate the presence of lighter 1^{-+} states, likely to be the states of two mesons into which the hybrid can decay. However, with the statistics available to us, we are unable to get convincing plateaus in the fits with more than one exponential in the 1^{-+} channel.

We performed a linear extrapolation in quark mass of the quenched results to the physical value of $(m_{\text{PS}}/m_{\text{V}})^2$. Because the calculations at the two quark masses were done on the same set of quenched configurations, they are highly correlated, and a single elimination jackknife method was used to estimate the statistical error of the extrapolation.

V. DISCUSSION AND CONCLUSIONS

There are several sources of systematic error to be estimated. The largest of these, namely use of the quenched approximation, is inextricably mixed with the problem of determining the overall scale, or lattice spacing, so we will discuss these issues together.

The first source of systematic error is due to the possibility of mixing of higher mass states in the 1^{-+} propagators. As described above we estimate this by looking at the mass range one might get by a reasonable variation of the fitting parameters.

We also have effects of finite lattice spacing. We obtained these results on lattices with $a \sim 0.09$ fm. For the conventional hadrons, we have masses at both $a \approx 0.13$ fm and $a \sim 0.09$ fm (Figs. 9 and 10). Since errors with this action are expected to be order $a^2 g^2$, and the finer lattice spacing is about $1/\sqrt{2}$ times the coarser lattice spacing, we expect that the difference between $a \sim 0.09$ fm and $a = 0$ masses is comparable to or slightly smaller than the difference between $a \sim 0.13$ and 0.09 fm. For the quenched $m_\rho/\sqrt{\sigma}$ and $m_N/\sqrt{\sigma}$ we see differences as large as 3% between the two lattice spacings, and a difference of about 2% in the ratio m_N/m_ρ at the light quark mass. Differences are smaller at the heavier mass — less than 1% in the nucleon to rho mass ratio. Therefore we expect effects of finite lattice spacing on our results based on hadron mass ratios to be around 1% for strange quarks, and we will use an estimate of 3% for light quarks.

The finite size of the entire lattice also introduces systematic error. The $28^3 \times 96$ lattice corresponds to a box $(2.5 \text{ fm})^3 \times 8.6 \text{ fm}$. In one case, three flavor QCD with light quark mass about 0.2 times the strange quark mass with a lattice spacing of 0.13 fm, we have calculated light hadron masses both in a 2.5 fm box and on a larger 3.6 fm spatial lattice. The ρ , ϕ and nucleon masses decrease by a barely significant 0.9(7)%, 0.25(25)% and 0.9(6)% respectively as the lattice size goes from 2.5 to 3.6 fm. Since these effects are expected to fall exponentially with lattice size, we can simply take these numbers as an estimate of the effect of the 2.5 fm box size on the light hadron masses. However, hybrids are expected to be rather extended objects and may feel the influence of a finite lattice more than smaller particles, so we will use an estimate of 2% for this systematic error.

The largest systematic errors come from use of the quenched approximation, from the choice of quantity used to set the lattice scale, and the necessity for an extrapolation to the physical value of the valence quark mass. These effects are interrelated and so must be

discussed together.

The hybrid mass estimates obtained above are in units of the inverse lattice spacing a^{-1} , so to convert these to physical units we need to know a . The lattice spacing is determined by calculating some quantity that is known from experiment. In other words, the simulation actually produces the ratio of the hybrid mass to some other dimensionful quantity. In a simulation with sea quark masses at their physical values, the choice of quantity to fix the lattice spacing would be just a question of convenience. However, in the quenched approximation, we will not get the real world values for ratios of masses, so there is an important choice to be made. Because it is easily measured, and because it does not require an extrapolation in valence quark masses, the static quark potential is often used to determine the lattice spacing. In particular, we may use the string tension, $\sqrt{\sigma} \approx 440$ MeV, the coefficient of the linear term in $V(r)$. We might also use $r_0 \approx 0.50$ fm or $r_1 \approx 0.34$ fm, which are defined by $r_x^2 F(r_x) = 1.65$ or 1.00 respectively. However, the shape of the static quark potential in quenched QCD differs from the shape with three dynamical flavors [21]. Hybrid mesons are expected to be large hadrons where the quarks are more likely to be in the linear part of the static quark potential, where σ is defined, rather than the region of crossover between Coulombic and linear behavior, where r_0 and r_1 are defined. This suggests that plotting results in units of the string tension might minimize (although by no means eliminate!) effects of quenching. This expectation is borne out by calculations of the conventional hadron spectrum with this same improved action, where using σ to define the lattice spacing produces better agreement of the quenched and three flavor results than using r_1 [21]. Figures 9 and 10 illustrate this with rho and nucleon masses plotted in units of r_1^{-1} and $\sqrt{\sigma}$ respectively. Since one of our important goals is to compare quenched and three flavor results, we therefore plot our results in units of the string tension. We also wish to compare our results with earlier results, and for this purpose the string tension in other published simulations is either available or can be reasonably estimated. In Fig. 11 we summarize our results along with the results of previous Wilson quark studies by the MILC collaboration [14], the UKQCD collaboration [13], the SESAM collaboration [16], as well as recent results from the Zhongshan University group [15] using Wilson quarks on an anisotropic lattice. We use the string tension σ to establish the lattice length scale and plot $M_{1-+}/\sqrt{\sigma}$. Our results are consistent with the earlier results at heavier quark masses.

To compare with experiment, we need to convert $M_H/\sqrt{\sigma}$ to physical units. Unfor-

unately, although phenomenological estimates are available, the string tension is not a parameter that is well known from experiment. The obvious workaround is to determine the string tension from the lattice results for $m_\rho/\sqrt{\sigma}$ etc., which in the end means that we are using the light hadron spectrum to set the length scale. Since ratios of quenched hadron masses are not quite those of the real world, we will get different estimates of the length scale depending on which hadron we choose. For the $s\bar{s}$ hybrid, the most reasonable choice for setting the length scale is a hadron with valence quark masses at the same value — the ϕ meson or Ω^- baryon, which means that we are essentially quoting M_H/M_ϕ or M_H/M_{Ω^-} with the quenched ϕ mass and Ω^- masses defined to be 1020 MeV and 1672 MeV. Estimating the masses of the conventional hadrons on our quenched lattices from a linear extrapolation of results at $am_q = 0.015$ and 0.030 , and setting the quenched string tension from the ϕ or Ω^- gives $\sqrt{\sigma} = 436(4)$ or $437(9)$ MeV respectively. (This remarkable agreement is surely coincidence, since other hadron mass ratios on these lattices differ by much larger amounts from the real world.) To estimate the light quark hybrid mass in MeV, we might use these estimates of $\sqrt{\sigma}$, or equally well argue that we should use light quark hadrons for comparison. Using the linearly extrapolated or interpolated ρ , K^* , N or Δ masses to set the scale gives quenched $\sqrt{\sigma}$ of 389(5), 410(4), 380(5) or 400(21) MeV respectively, showing statistical errors only. These estimates are in reasonable agreement with phenomenological estimates from potential models on charmonium and bottomonium spectroscopy; for example $\sqrt{\sigma} = 384$ MeV or 427 MeV in Refs. [22] and [23] respectively. Thus in estimating light quark hybrid masses in MeV we might consider a range of possible values for the quenched $\sqrt{\sigma}$ from around 380 to 440 MeV.

We begin with estimates for the $s\bar{s}$ hybrid masses. As mentioned above, it seems most consistent to use masses of hadrons made from strange quarks to set the lattice spacing in this case. If we use the ϕ meson to set the length scale, using the results in Tables I and II we find, with statistical error only

$$M_{H,s\bar{s}} = 1020 \text{ MeV} \left(\frac{1.062(12)}{0.523(3)} \right) = 2071(26) \text{ MeV} \quad . \quad (6)$$

Systematic errors include fit choice, nonzero lattice spacing, finite spatial size, and effects of quenching. The first three have been discussed above. Effects of quenching can be estimated in part from the variation of our mass estimates among different ways of fixing the lattice scale, and in part from differences of other hadronic ratios between full and quenched QCD,

as for example in Fig. 10. Here we include what we expect is a fairly conservative 5% error for this effect, thus estimating

$$M_{H,s\bar{s}} = 2071(26)(39)(1\%)(2\%)(5\%) \quad (7)$$

$$= 2071(120) \text{ MeV} \quad , \quad (8)$$

where the errors are statistical, fit choice, lattice spacing, box size and quenching respectively.

A similar calculation using the Ω^- mass to set the scale gives

$$\begin{aligned} M_{H,s\bar{s}} &= 1672 \left(\frac{1.062(12)}{0.855(17)} \right) \\ &= 2077(48)(39)(1\%)(2\%)(5\%) \\ &= 2077(129) \text{ MeV} \quad . \end{aligned} \quad (9)$$

We might also use the mass of a fictional octet baryon made from three quarks with the mass of the strange quark, assigning it a mass of $M_{sss} = m_N + \frac{3}{2}(m_{\Xi} - m_N) = 1507 \text{ MeV}$:

$$\begin{aligned} M_{H,s\bar{s}} &= 1507 \left(\frac{1.062(12)}{0.771(2)} \right) \\ &= 2075(24)(39)(1\%)(2\%)(5\%) \\ &= 2075(119) \text{ MeV} \quad . \end{aligned} \quad (10)$$

These three estimates are in remarkably close, and doubtless partly fortuitous, agreement.

Repeating this calculation with the three flavor lattices with $m_{u,d} = m_s$ with the ϕ , Ω^- and sss baryon setting the scale produces

$$\begin{aligned} M_{H,s\bar{s}} &= 1020 \left(\frac{0.986(30)}{0.4778(9)} \right) \\ &= 2105(64)(64)(1\%)(2\%)(3\%) \\ &= 2105(120) \text{ MeV} \end{aligned} \quad (11)$$

$$\begin{aligned} M_{H,s\bar{s}} &= 1672 \left(\frac{0.986(30)}{0.7659(24)} \right) \\ &= 2152(66)(66)(1\%)(2\%)(3\%) \\ &= 2152(123) \text{ MeV} \end{aligned} \quad (12)$$

$$\begin{aligned} M_{H,s\bar{s}} &= 1507 \left(\frac{0.986(30)}{0.6991(10)} \right) \\ &= 2125(65)(65)(1\%)(2\%)(3\%) \\ &= 2125(121) \text{ MeV} \end{aligned} \quad (13)$$

respectively. Here we have assigned an error of 3% for the partial quenching, or the remaining extrapolation of the sea quark masses to their physical values. Finally, we made an estimate of the $s\bar{s}$ hybrid mass from the run with $m_{u,d} = 0.4m_s$. Although the error on this estimate, mostly coming from the choice of fit range, is too large for it to be very useful, we include it for completeness.

$$\begin{aligned}
M_{H,s\bar{s}} &= 1020 \left(\frac{0.911(34)}{0.4792(16)} \right) \\
&= 1939(73)(213)(1\%)(2\%)(2\%) \\
&= 1939(233) \text{ MeV} .
\end{aligned} \tag{14}$$

Since the sea quarks here are much lighter, we used 2% as our estimate of the systematic error from partial quenching in this number. We can summarize this with an estimate of 2100 ± 120 MeV for the mass of the $s\bar{s}$ 1^{-+} hybrid meson.

To estimate the mass of a light quark 1^{-+} hybrid meson we use the jackknife extrapolation of the quenched results to $(m_{PS}/m_V)^2 = 0.033$, $am_H = 0.919(39)$. If we use the ϕ to set the scale, this would correspond to a mass of

$$\begin{aligned}
M_{H,u\bar{u}} &= 1020 \left(\frac{0.919(39)}{0.523(3)} \right) \\
&= 1792(77)(36)(3\%)(2\%)(5\%) \\
&= 1792(139) \text{ MeV} ,
\end{aligned} \tag{15}$$

with similar results using the Ω^- or sss baryon. However, if we were to use the smaller estimates of the string tension obtained from linear extrapolations of light quark hadron masses to the physical light quark mass, we would obtain smaller values around 1600 MeV. As discussed above we have assigned a larger 3% systematic error for the effect of nonzero lattice spacing. We have also assigned a larger 5% error from quenching and chiral extrapolation. One reason that a larger systematic error is required here is that we are estimating the lattice spacing in large part from hadrons made up of strange quarks. Our strange quark mass was fixed by tuning the pseudo-scalar to vector meson mass ratio, and would have come out slightly different if we had used some other quantity. The effect of uncertainty in fixing the strange quark mass mostly cancels from mass ratios of hadrons made up of strange quarks, such as $M_{H,s\bar{s}}/M_\phi$, but will be present when quantities such as M_ϕ are used in estimating the mass of light quark hadrons. More evidence that this larger systematic error is required is seen in the extrapolations of conventional hadron masses to the physical light quark mass.

If a naive linear extrapolation is made, and the resulting masses used to set the scale for the 1^{-+} hybrid mass, the close agreements of the scales from various conventional hadrons that we found when using hadrons made from strange quarks is no longer present, as seen in the string tension estimates above.

Given the systematic errors from quenching and chiral extrapolation, our estimate for the mass of the light quark 1^{-+} meson is not inconsistent with the experimental candidate $\pi_1(1600)$. In Fig. 11 we include the 1^{-+} experimental candidates $\pi_1(1400)$ and $\pi_1(1600)$ at the physical value of $(m_{\text{PS}}/m_V)^2 = (m_\pi/m_\rho)^2 = 0.033$. These particles are represented by vertical bars, offset slightly to the left or right for clarity, representing the range of values for the quenched string tension from 380 to 440 MeV.

The $m_{u,d} = 0.4m_s$ data illustrates that dynamical quarks introduce new and significant processes that contribute to the 1^{-+} propagator. On this same set of lattices, mass fits for stable hadrons, even with $ma = 0.0124$ valence quarks, display plateaus as functions of minimum included distance, D_{min} with fixed maximum distance, D_{max} . The plateaus are similar for quenched and full QCD. In contrast, for the 1^{-+} , the full QCD fits do not show even the shorter plateau found in the quenched fits. We illustrate this by comparing fit plots for quenched and full QCD hybrids and nucleons in Figure 12. Fit plots for nucleon and quenched hybrids show a plateau, indicating the propagator has a single exponential form in the region D_{min} to D_{max} . The full QCD hybrid fit plot deviates from a plateau in a significant manner — at minimum distance five, in the range which we have generally used for our quoted mass estimate, the low mass full QCD fits drop to a smaller value. Though quenching often introduces a systematic effect in the mass, this propagator is different in a way that suggests mixing of more than one exponential, representing propagators of different states with $J^{PC} = 1^{-+}$. Our hybrid propagators with light, dynamical quarks show features that are not evident either in hybrid propagators with heavier or quenched quarks, or in stable hadron propagators even with light dynamical quarks.

Four-quark states, molecular states of two mesons, or two independent mesons can have $J^{PC} = 1^{-+}$ without the gluonic excitations. For example the combination of $b_1 + \pi$ can give 1^{-+} with $I = 1$, and as the sum of these masses is less than the predicted mass of the lowest 1^{-+} hybrid, we expect that dynamical quarks introduce the possibility of the hybrid decaying into this two-meson state. In fact, at the values of the quark masses that we used the 1^{-+} energies found in our dynamical simulations, while similar to the quenched

hybrid masses, are also very close to the expected decay channel masses. For the run with three degenerate sea quarks at m_s , our 1^{-+} mass is $am_H = 0.97(3)(3)$, very close to the sum of the “ π ” and “ b_1 ” masses: $am_\pi + am_{b_1} = 0.32 + 0.68 = 1.00$. For the run with $m_{u,d} = 0.4m_s$, we would expect decays into a pseudo-scalar K and a P-wave strange meson - a K_1 . Again, our estimated mass for the $s\bar{s} 1^{-+}$, $am_H = 0.90(4)(10)$, is close to the sum $am_K + am_{K_1} = 0.27 + 0.63 = 0.90$.

We now have ahead of us the task of understanding these contributions so that we can make useful predictions of the 1^{-+} hybrid mass in the presence of dynamical quarks. It is clear from our results with dynamical quarks that it will not be sufficient to simply do the same analysis that was done on the quenched gauge configurations, simply replacing them with full QCD configurations. One obvious avenue that may shed some light is to measure cross-correlators between the $\rho \times B$ operator and the two-meson state, as was explored with Wilson quarks in Ref. [14]. A more detailed study along these lines in the static quark (heavy quark) limit has been done by the UKQCD collaboration [24]. It may also be useful to study the dependence of the exotic energy as a function of valence quark mass (possibly with fixed sea quark mass) to look for an avoided level crossing as the decay threshold is crossed, as was done for the non-exotic 0^{++} meson in Ref. [21].

ACKNOWLEDGEMENTS

Computations for this work were performed at the San Diego Supercomputer Center (SDSC), the Pittsburgh Supercomputer Center (PSC), Oak Ridge National Laboratory (ORNL) and the National Energy Resources Supercomputer Center (NERSC). This work was supported by the U.S. Department of Energy under contracts DOE – DE-FG02-91ER-40628, DOE – DE-FG02-91ER-40661, DOE – DE-FG02-97ER-41022 and DOE – DE-FG03-95ER-40906 and National Science Foundation grants NSF – PHY99-70701 and NSF – PHY00-98395.

-
- [1] D. Alde *et al.*, Phys. Lett. B **205** (1988) 397; D. R. Thompson *et al.*, Phys. Rev. Lett. **79** (1997) 1630; S.U. Chung *et al.*, Phys. Rev. D **60** (1999) 092001; A. Abele *et al.*, Phys. Lett. B **423** (1998) 175; A. Abele *et al.*, Phys. Lett. B **446** (1999) 349.

- [2] G. S. Adams *et al.*, Phys. Rev. Lett. **81** (1998) 5760; E. I. Ivanov *et al.*, Phys. Rev. Lett. **86** (2001) 3977; Y. P. Gouz *et al.*, In **Dallas 1992, Proc., HEP, vol. 1** 572-576.
- [3] T. Barnes, F. E. Close and E. S. Swanson, Phys. Rev. D **52**, 5242 (1995)
- [4] M. Flensburg, C. Peterson and L. Sköld, Z. Phys. C **22**, 293 (1984)
- [5] T. Barnes, F. E. Close and F. deViron, Nucl. Phys. B **224**, 241 (1983).
- [6] M. Chanowitz and S. R. Sharpe, Nucl. Phys. B **222**, 211 (1983).
- [7] T. Barnes and F. E. Close, Phys. Lett. B **116**, 365 (1982).
- [8] T. Barnes, Nucl. Phys. B **158**, 171 (1979).
- [9] K. G. Chetyrkin and S. Narison, Phys. Lett. B **485**, 145 (2000).
- [10] J. M. Cornwall and S. F. Tuan, Phys. Lett. B **136**, 110 (1984).
- [11] J. I. Latorre, P. Pascual and S. Narison, Z. Phys. C **34**, 347 (1987).
- [12] S. Narison, Nucl. Phys. A **675**, 54C (2000).
- [13] P. Lacock, C. Michael, P. Boyle and P. Rowland, Phys. Lett. B **401** (1997) 308.
- [14] C. Bernard *et al.*, Phys. Rev. D **56** (1997) 7039; C. Bernard *et al.*, Nucl. Phys. (Proc. Suppl.) **60A** (1998) 61.
- [15] Z.H. Mei and X.Q. Luo, [arXiv:hep-lat/0206012]; to appear in Nucl. Phys. B (Proc. Suppl.) [hep-lat/0209049].
- [16] P. Lacock and K. Schilling (SESAM collaboration), Nucl. Phys. (Proc. Suppl.) **73** (1999) 261.
- [17] C. Bernard *et al.*, hep-lat/0209097, to appear in Nucl. Phys. B(Proc. Suppl.).
- [18] M. F. Golterman, Nucl. Phys. B **273**, 663 (1986).
- [19] M. Falcioni, M.L. Paciello, G. Parisi and B. Taglienti, Nucl. Phys. B **251** (1985) 624; M. Albanese *et al.*, Phys. Lett. B **192** (1987) 163.
- [20] K. Orginos and D. Toussaint, Phys. Rev. D **59** (1999) 014501; K. Orginos, D. Toussaint and R. L. Sugar, Phys. Rev. D **60** (1999) 054503; K. Orginos, R. Sugar and D. Toussaint, Nucl. Phys. (Proc. Suppl.) **83** (2000) 878 ; [arXiv:hep-lat/9909087]. G. P. Lepage, Phys. Rev. D **59** (1999) 074502, [arXiv:hep-lat/9809157].
- [21] C. Bernard *et al.*, Phys. Rev. D **64** (2001) 054506; C. Bernard *et al.*, [arXiv:hep-lat/0208041], to appear in Nucl. Phys. B(Proc. Suppl.); C. Bernard *et al.*, in progress.
- [22] J.L. Richardson, Phys. Lett. **82B**, 272 (1979).
- [23] E. Eichten *et al.*, Phys. Rev. D **21**, 203 (1980).
- [24] C. McNeile, C. Michael and P. Pennanen (UKQCD Collaboration), Phys. Rev. D **65** (2002)

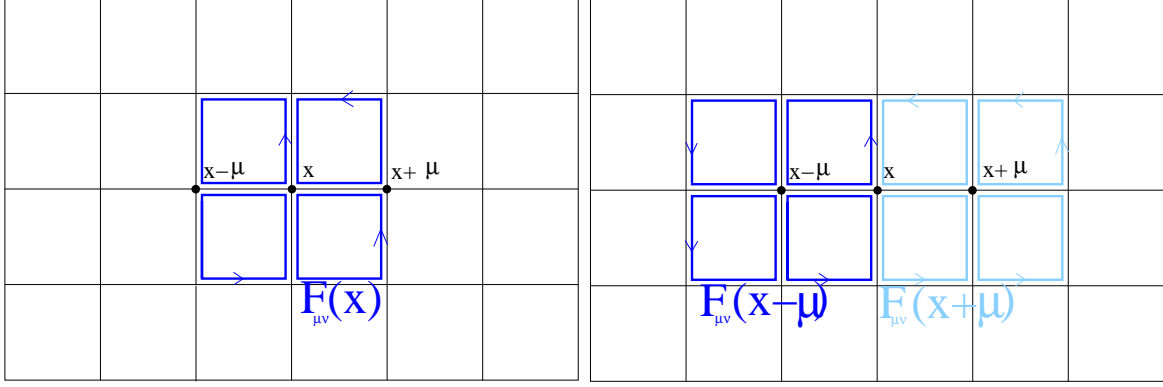


FIG. 1: Chromomagnetic field measured at the site of the antiquark (left) and the quark (right).

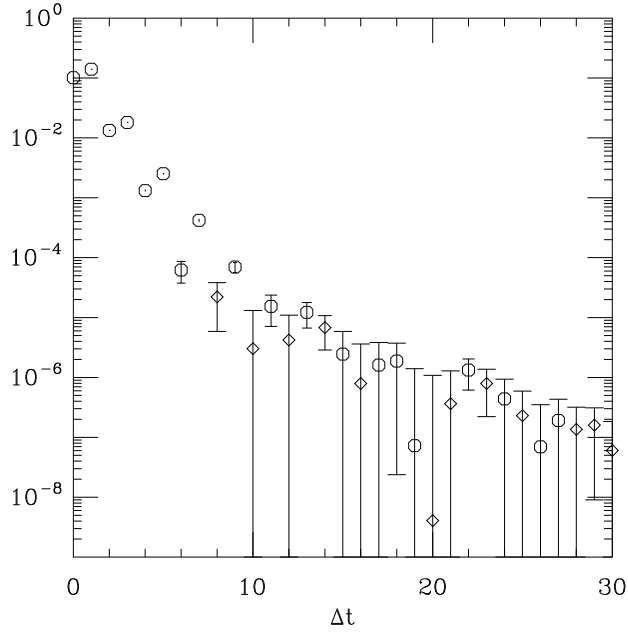


FIG. 2: Propagator for quenched lattice with $10/g^2 = 8.40$, $ma=0.016$. Octagons represent positive values, diamonds represent negative values.

094505.

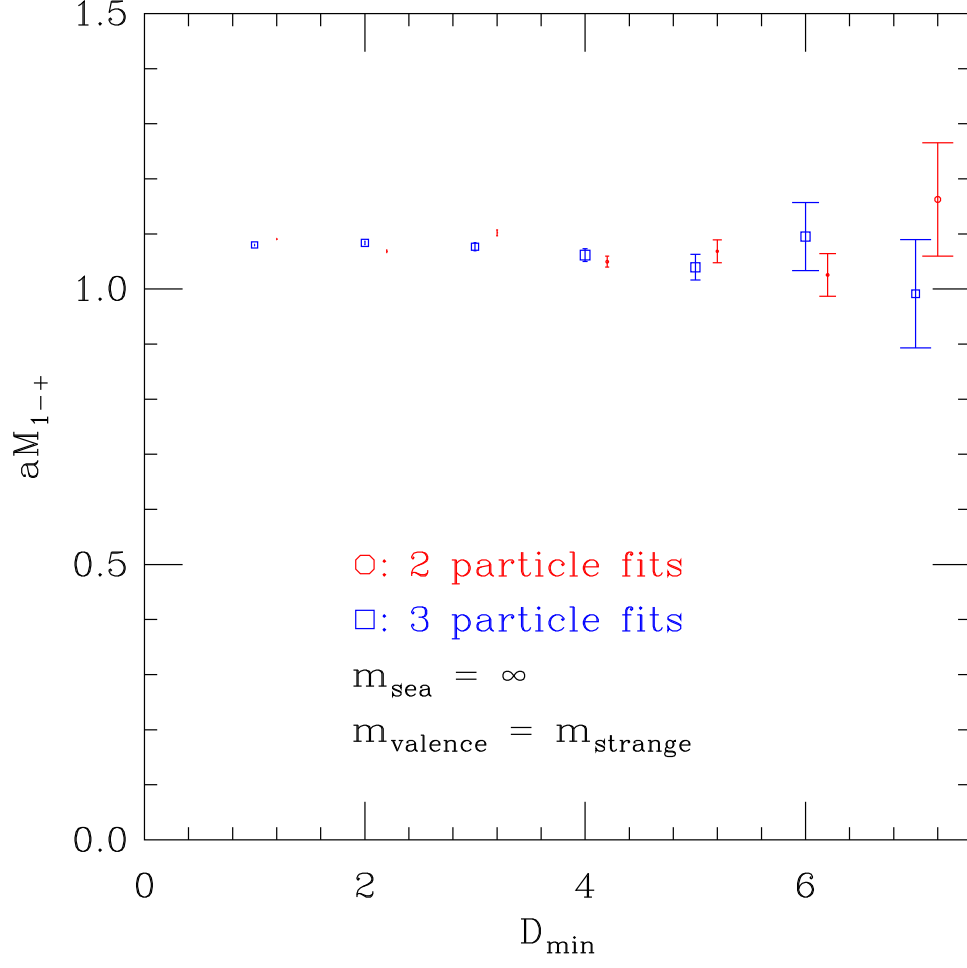


FIG. 3: aM_{1-+} vs. D_{\min} for $10/g^2 = 8.40$ quenched lattices $am_{\text{valence}} = 0.040$. The octagons are four parameter fits, with one mass and amplitude of each parity, and the squares are five parameter fits with one 1^{++} mass fixed to the a_1 mass, as described in the text. All these fits used a maximum distance $D_{\max} = 15$. The four parameter fit points are shifted slightly to the right for clarity. The symbol size is proportional to the confidence level of the fit, with the symbol size in the labels corresponding to 50%.

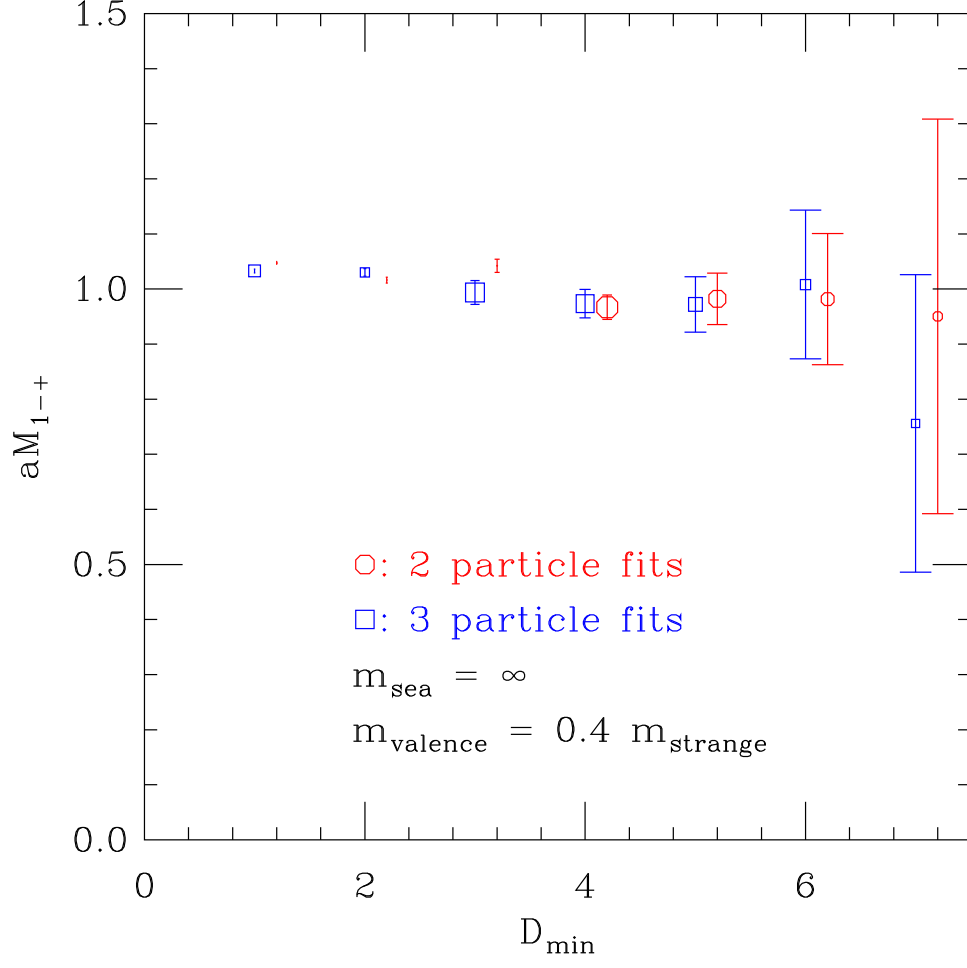


FIG. 4: aM_{1-+} vs. D_{\min} for $10/g^2 = 8.40$ quenched lattices with $am_{\text{valence}} = 0.016$, using $D_{\max} = 15$. Notation is the same as in Fig. 3.

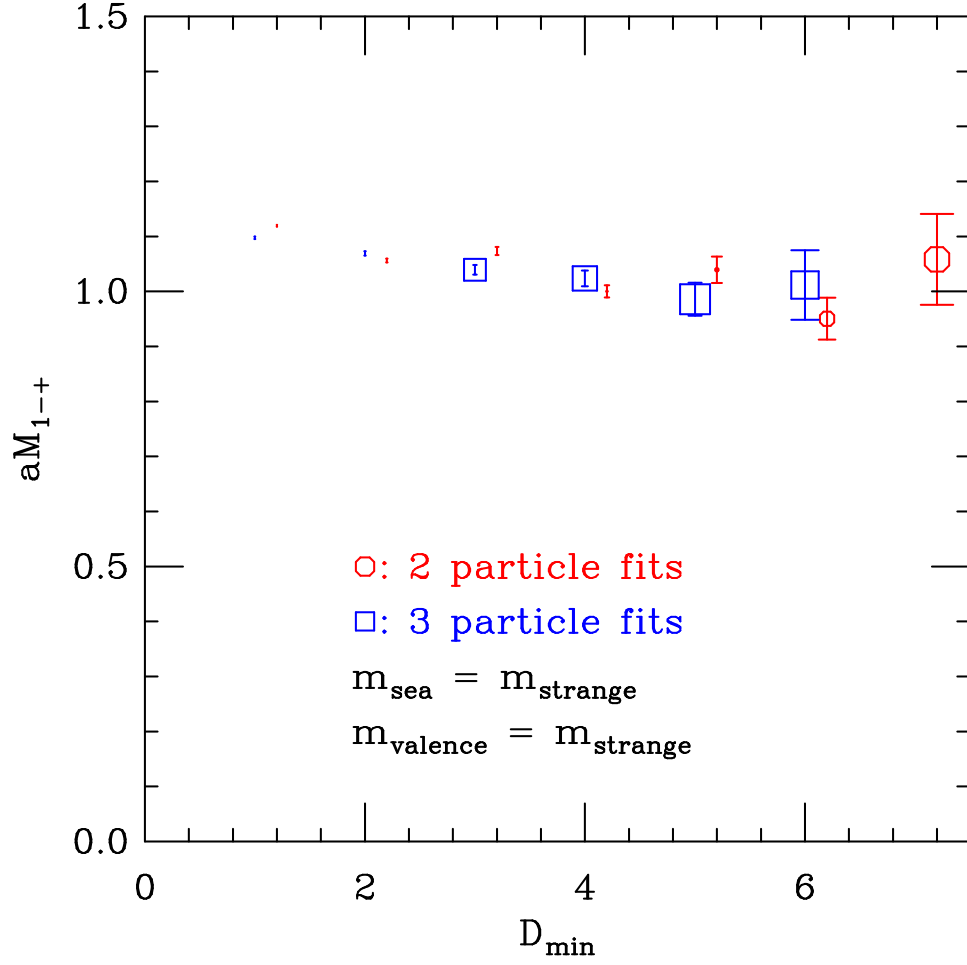


FIG. 5: aM_{1-+} vs. D_{\min} for $10/g^2 = 7.18$ with three degenerate dynamical quarks with mass $am_{\text{sea}} = am_{\text{valence}} = 0.031$, using $D_{\max} = 15$. Notation is the same as in Fig. 3.

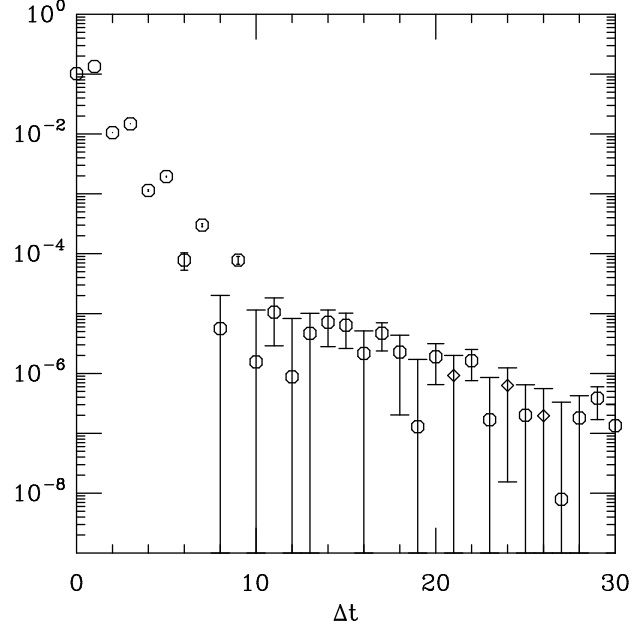


FIG. 6: Propagator for three flavor lattice with $10/g^2 = 7.11$, $ma=0.0124$. Octagons represent positive values, diamonds represent negative values.

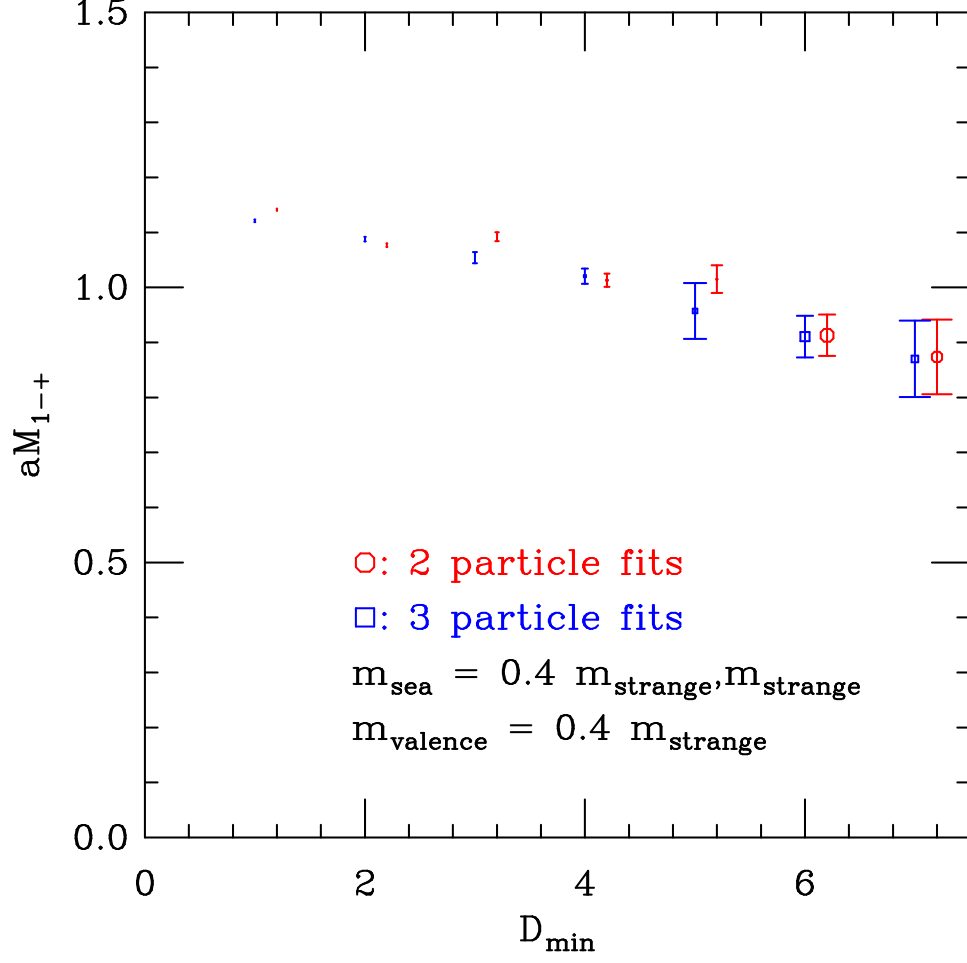


FIG. 7: aM_{1-+} vs. D_{\min} for $10/g^2 = 7.11$ with three dynamical quarks with masses $am_{\text{light}} = 0.0124$ and $am_{\text{heavy}} = 0.031$. The valence quark mass is $am_{\text{valence}} = 0.031$. Notation is the same as in Fig. 3.

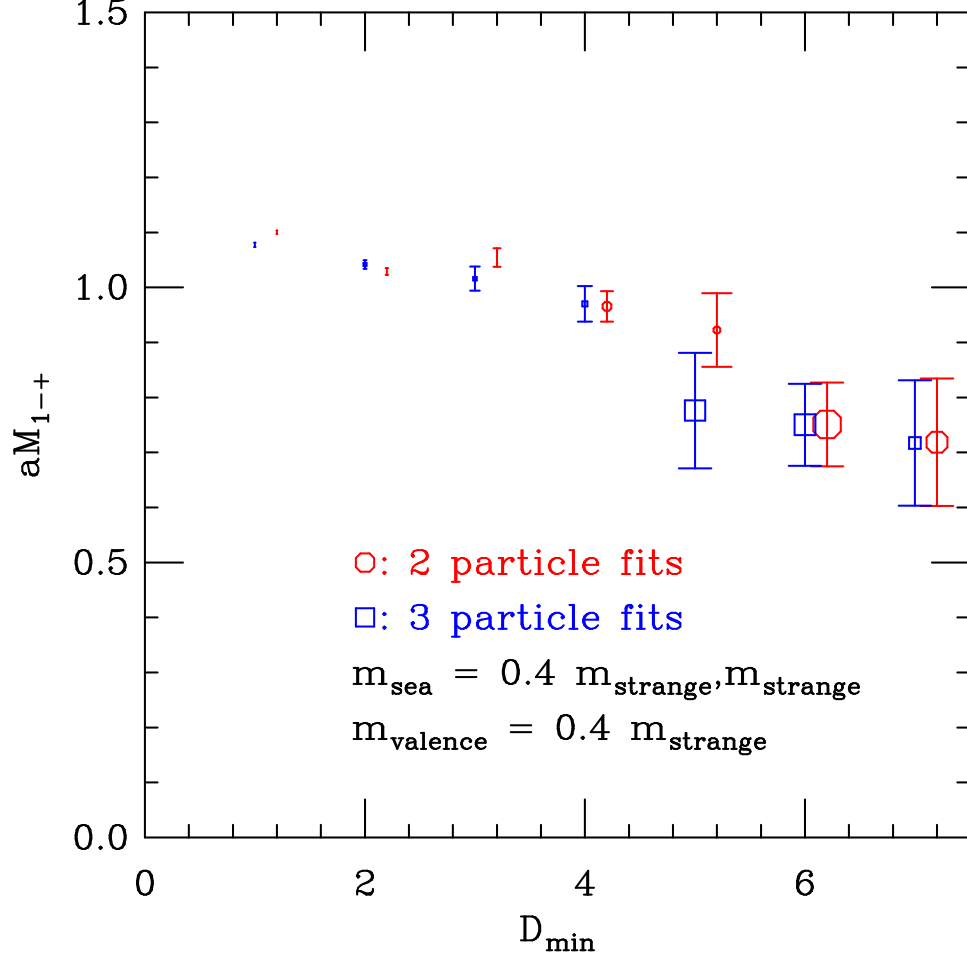


FIG. 8: aM_{1-+} vs. D_{\min} for $10/g^2 = 7.11$ with three dynamical quarks with masses $am_{\text{light}} = 0.0124$ and $am_{\text{heavy}} = 0.031$. The valence quark mass is $am_{\text{valence}} = 0.0124$. Notation is the same as in Fig. 3.

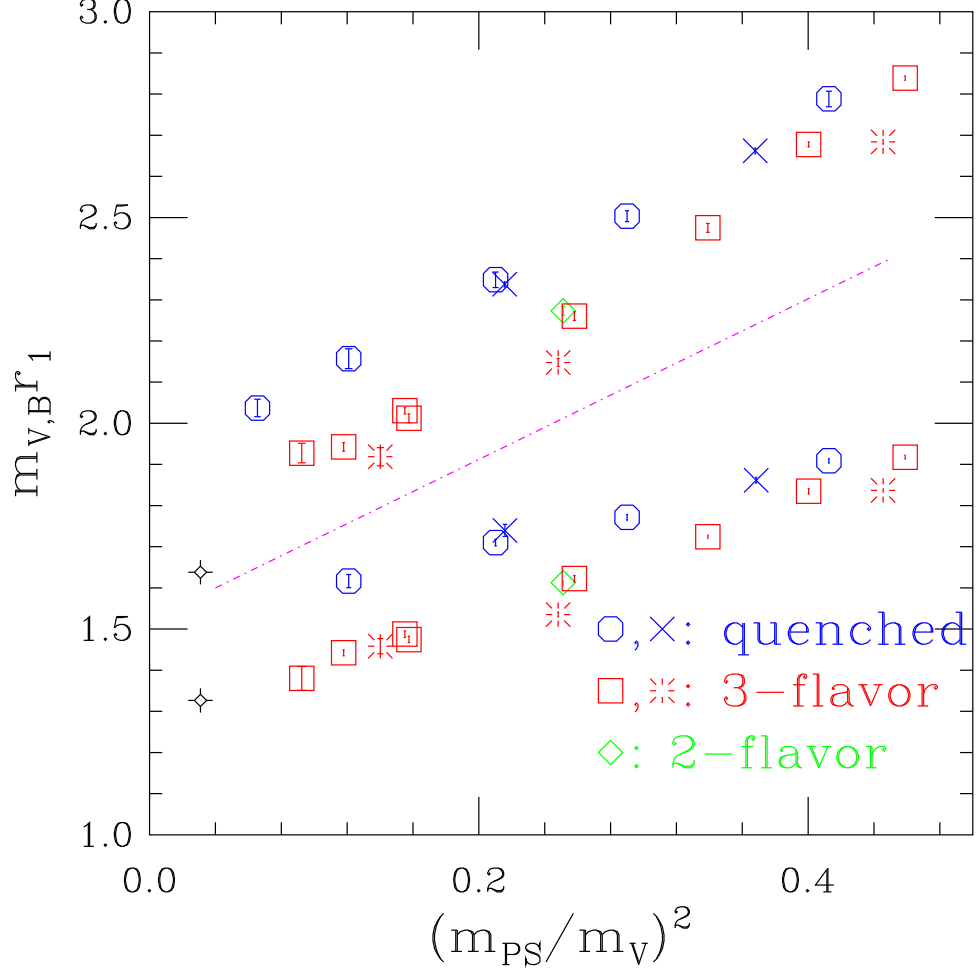


FIG. 9: Vector meson (“V”) and octet baryon (“B”) masses in units of r_1 , which is defined from the static quark potential by $r_1^2 F(r_1) = 1.0$. This graph contains points from quenched simulations with $a \approx 0.13$ fm (octagons) and 0.09 fm (crosses), and from simulations with three flavors of dynamical quarks (two light and one strange quark) at $a \approx 0.13$ fm (squares) and 0.09 fm (bursts). The diamond is from a two flavor simulation with $a \approx 0.13$ fm. Points above the dashed line are baryon masses, and those below the dashed line vector meson masses.

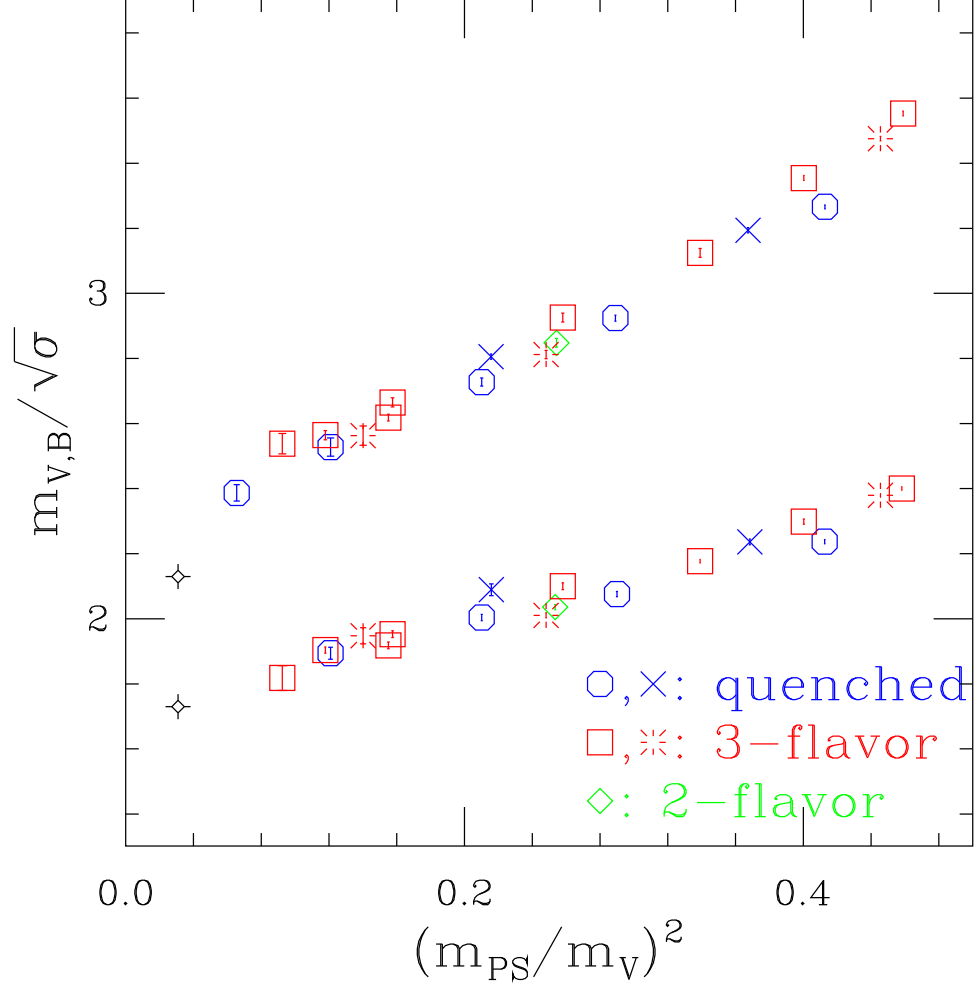


FIG. 10: Vector meson (“V”) and octet baryon (“B”) masses in units of the square root of the string tension. The meaning of the symbols is the same as in Fig. 9

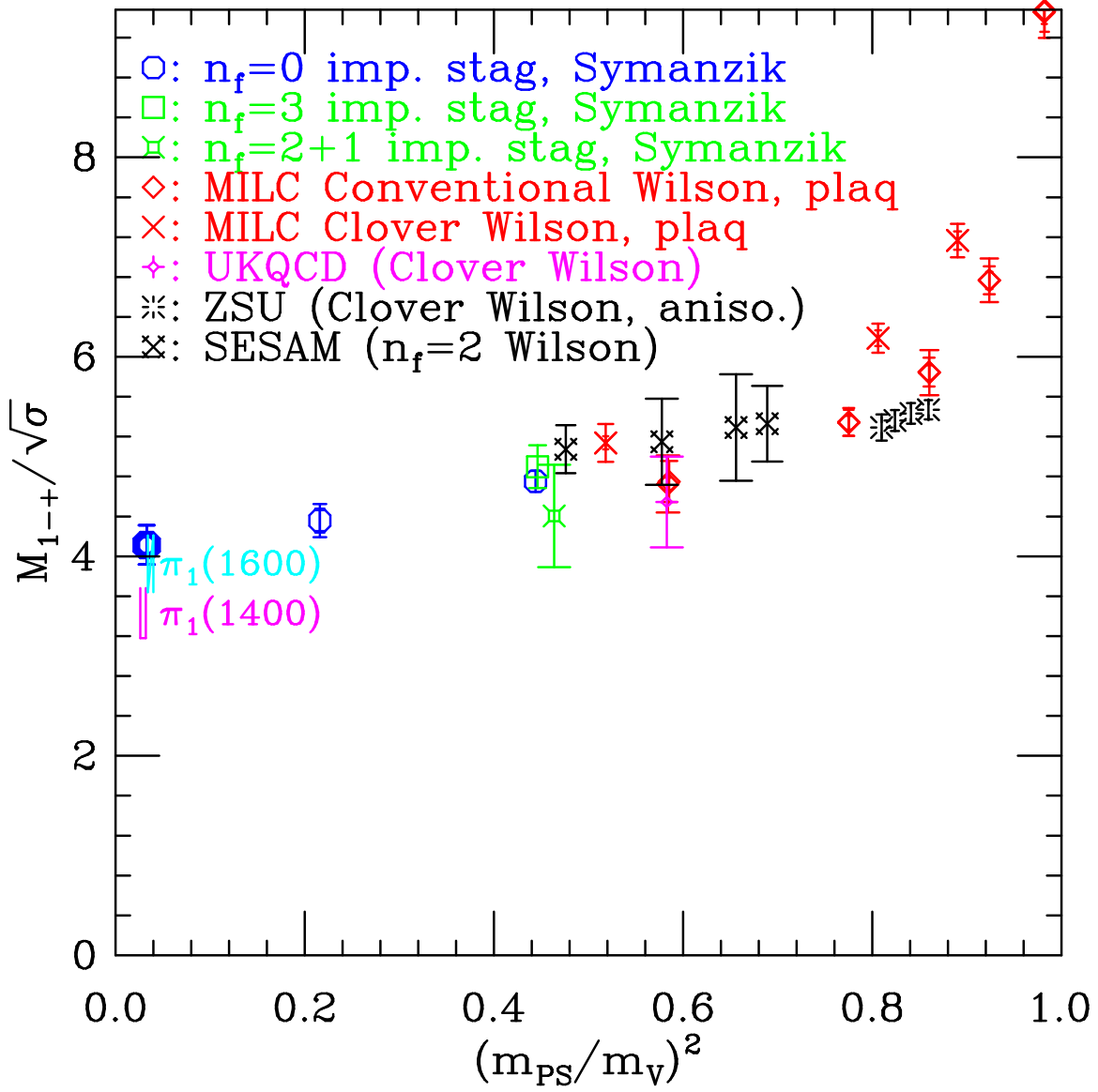


FIG. 11: Summary of 1^{-+} hybrid meson mass predictions as a function of $(m_{PS}/m_V)^2$. The bold octagon represents the linear extrapolation of $n_f = 0$ data to $(m_{PS}/m_V)^2 = 0.033$. The improved staggered points are from this work, while the earlier data is from Refs [13, 14, 15, 16]

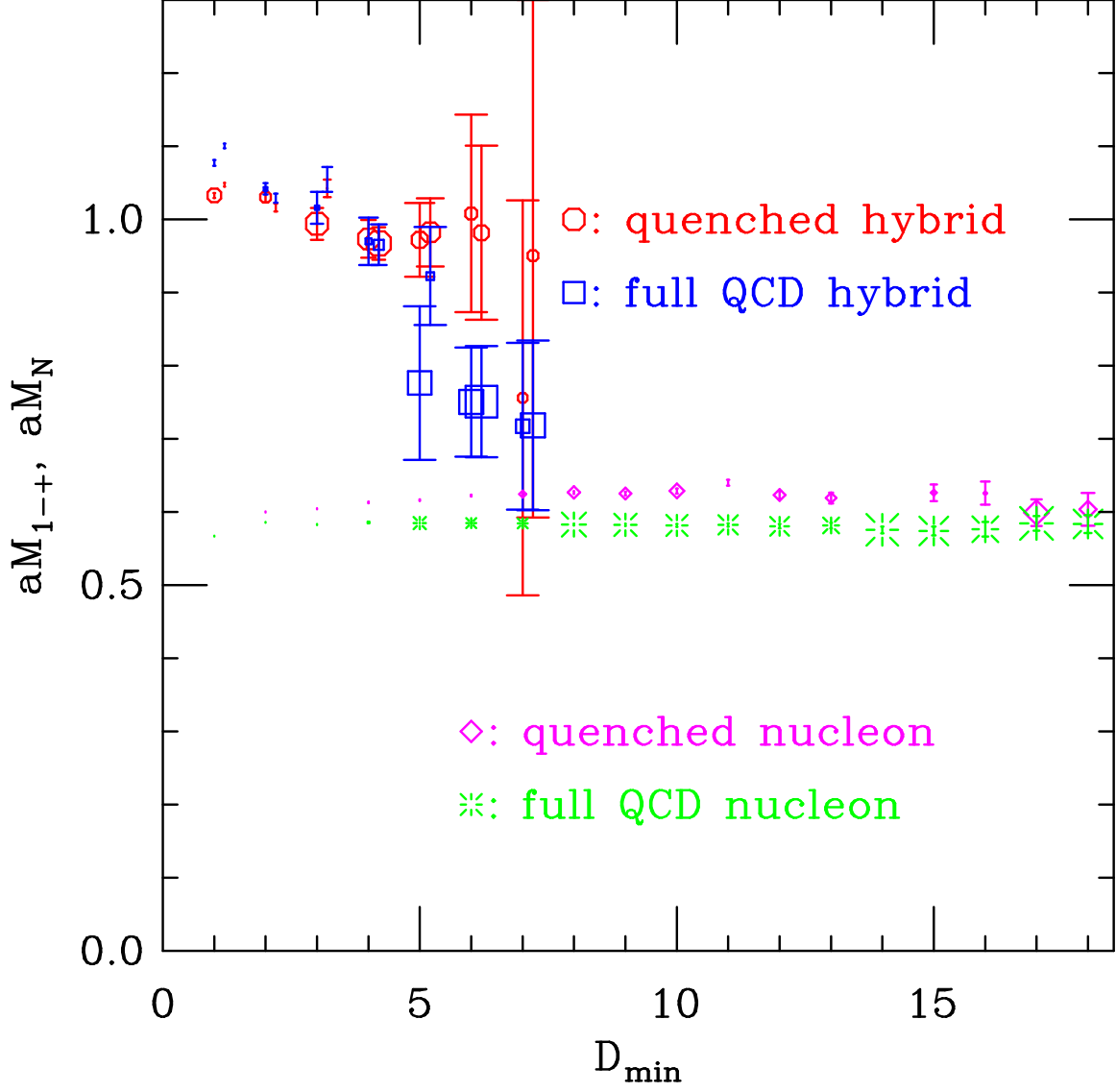


FIG. 12: Hybrid and nucleon mass fits in quenched and full QCD with light dynamical quark mass $am_{\text{light}} \approx 0.4m_s$. The valence quark mass is about $0.4m_s$, which is $am_{\text{valence}} = 0.016$ for the quenched case and 0.0124 for the three flavor case.